http://dx.doi.org/10.21577/0103-5053.20180133

J. Braz. Chem. Soc., Vol. 29, No. 12, 2542-2553, 2018
Printed in Brazil - ©2018 Sociedade Brasileira de Química

Article

β-Enaminoesters as Novel Corrosion Inhibitors for Carbon Steel in Acidic Medium

Mariana F. L. P. Carlos,[a] Arthur Valbon,[a] Marcelo A. Neves,[b] Margareth R. L. Santos[a] and Aurea Echevarria[*,a]*

[a]*Departamento de Química, Instituto de Ciências Exatas, Universidade Federal Rural do Rio de Janeiro, 23851-970 Seropédica-RJ, Brazil*

[b]*Departamento de Física, Instituto de Ciências Exatas, Universidade Federal Rural do Rio de Janeiro, 23851-970 Seropédica-RJ, Brazil*

In this work, two β-enaminoesters, EN1 and EN2, were synthesized, characterized and their anticorrosion effects on American Iron and Steel Institute (AISI) 1020 carbon steel in 0.5 mol L^{-1} HCl were investigated using gravimetric and electrochemical methods. The results revealed that both compounds inhibit corrosion. Good correlations were observed between results obtained for gravimetric and electrochemical methods. EN1 exhibited highest efficiency of 98% after 24 h of immersion in HCl solution. The adsorption of compounds on steel surface followed the modified Langmuir adsorption isotherm. Surface morphology of carbon steel was examined using scanning electron microscopy showing that the metal surface was protected by EN1 as inhibitor of corrosion.

Keywords: corrosion, β-enaminoesters, EIS, LRP, mass loss

Introduction

Among the various metallic materials that can suffer corrosion, carbon steel is widely used in several industrial segments because it is easier to handle and more cost-effective than more noble materials, and approximately 20% of steel produced is intended for the replacement of parts for corroded equipment, parts or installations. The petroleum and petrochemical industries suffer the most attacks of corrosive agents, causing damages in the entire productive chain, from extraction to refining.[1] Acidic solutions are usually used in industries, such as pickling, acid cleaning and the cleaning of oil refinery equipment, even though they are increasing the corrosion of metallic materials and affect the performance of metals subjected to such processes.[2]

The knowledge and characterization of the different aggressive means responsible for the chemical and electrochemical reactions that provoke the deterioration of the materials are of fundamental importance so that increasingly effective methods to combat the corrosion can be developed.[3] One of the methods used to prevent corrosion is the use of corrosion inhibitors.

Such inhibitors are organic or inorganic substances, which, when added to the corrosive medium, prevent or reduce the development of corrosion reactions. These inhibitors are usually adsorbed, making a very thin and persistent film, which leads to a decrease in the corrosion rate, due to the slowing of the anodic or cathodic reactions (or both).[4]

The use of organic compounds to inhibit metallic corrosion in acidic media is well established. Compounds containing electron-donating atoms, such as oxygen, nitrogen and sulfur, have shown efficiency as carbon steel corrosion inhibitors. The molecular structure, aromaticity and the presence of π electrons or non-ligand electron pairs are important characteristics to determine how these molecules adsorb on the metal surface and, when adsorbed, how they block the active sites and reduce the corrosion rate.[5,6]

The general term "enaminone" refers to any compound having the N–C=C–C=O conjugate system. Enaminones are β-enaminocarbonyl compounds, derivatives of β-diketones, β-ketoesters and other β-dicarbonyl compounds. The most common representatives of this class are β-enaminoketones and β-enaminoesters.[7,8] Enaminoesters possess structures with acceptor-donor electronic effects, and due to the mesomeric effect of the acyl and amino substituents on the double bond, the delocalization of π electrons resulting from this effect leads to a remarkable polarization of these olefinic carbons, giving these compounds a distinct reactive nature.[9]

*e-mail: echevarr@ufrrj.br

Schiff bases are similar compounds that have good corrosion inhibition efficiencies because they have the necessary characteristics for interactions with metals. Recently, Prajila and Abraham[10] studied the anticorrosive activity of three Schiff bases against carbon steel, being observed 94% of corrosion inhibition efficiency for (4-(4-hydroxybenzylideneamino)-4*H*-1,2,4-triazole-3,5-diyl)dimethanol in the concentration of 1.6×10^{-4} mol L^{-1}, 95% for (4-(4-methoxybenzylideneamino)-4*H*-1,2,4-triazole-3,5-iyl)dimethanol (1.5×10^{-4} mol L^{-1}) and 97% for (4-(3,4-dimethoxybenzylideneamino)-4*H*-1,2,4-triazole-3,5-diyl)dimethanol (1.4×10^{-4} mol L^{-1}), by electrochemical impedance spectroscopy (EIS) method in 0.5 M HCl.[10]

Heydari *et al.*[11] also investigated as corrosion inhibitors, for mild steel, other two Schiff bases: *N*-(4-methoxybenzylidene)-2-[2-((*E*)-2-(4-methoxybenzylideneamino)phenyl) disulfanyl]benzenemine and *N*-(4-nitrobenzylidene)-2-[2-((*E*)-2-(4-nitrobenzylideneamino)phenyl)disulfanyl] benzenemine, with 97 and 88%, in 1.0×10^{-3} and 9.7×10^{-5} mol L^{-1} of concentrations, respectively, by weight loss method in 1 M HCl.[11]

Thus, due to some structural similarities, enaminoesters are compounds considered to be potential corrosion inhibitors. Although these compounds are known, there are no reports in the literature of the use of these compounds as corrosion inhibitors, so this application is unprecedented. Therefore, in this work we presented the synthesis and the investigation of the inhibitory effects of two β-enaminoesters (EN1 and EN2) on American Iron and Steel Institute (AISI) 1020 carbon steel in 0.5 mol L^{-1} HCl, employing potentiodynamic polarization (PP), linear polarization resistance (LPR), EIS, mass loss and scanning electron microscopy (SEM).

Experimental

Materials and instruments

^{1}H and ^{13}C nuclear magnetic resonance (NMR) spectra were obtained on Bruker NMR Ultrashield 500 MHz spectrometer, with tetramethylsilane as the internal reference and $CDCl_3$ or DMSO-d_6 as the solvent; the chemical shifts (δ) are reported as ppm. Peak multiplicities are expressed as follows: s, singlet; d, doublet; t, triplet; q, quartet. Coupling constants (*J* values) are given in hertz (Hz). Elemental analyses were performed on a PerkinElmer 2400 CHN at the Laboratory of Environmental Science of the Universidade Estadual do Norte Fluminense (UENF). Reactions were monitored by thin-layer chromatography (TLC) on Merck silica gel 60 F254 aluminum sheets. TLC spots were visualized by inspection of the plates under UV light (254 and 365 nm). The reagents and solvents were purchased from Sigma-Aldrich and Vetec, respectively. All reagents were used without any further purification. The water used in all experiments was MilliQ level.

Synthesis

Preparation of the ethyl-(2*Z*)-3-[(2-phenylethyl)amino]but-2-enoate (EN1) and ethyl-(2*Z*)-3-{[2-(4-methoxyphenyl) ethyl]amino}but-2-enoate (EN2)

Ethyl acetate was treated with *p*-toluene sulfonic acid (*p*-TSA) in the presence of ethanol as a solvent. After 10 min in magnetic stirring, phenethylamine or *p*-phenethylamine and molecular sieves were added. The mixture was stirred at 30 °C for 20 h.[12,13] Then, the molecular sieves were filtered and the ethanol was evaporated. Dichloromethane and saturated aqueous $NaHCO_3$ solution were added to the mixture until neutrality. The organic phase was dried with Na_2SO_4 and filtered; then, the solvent was evaporated, and the product was collected. EN1 was obtained with a 74% yield, and EN2 with an 84% yield. The synthetic route is shown in Figure 1.

Ethyl-(2*Z*)-3-[(2-phenylethyl)amino]but-2-enoate (EN1)

Light yellow oil; n_p^a = 1.549; ^{1}H NMR (500 MHz, $CDCl_3$) δ 8.67 (s, 1H, H-7), 7.33 (m, 2H, H-2), 7.23 (m, 2H, H-4), 4.45 (s, 1H, H-9), 4.10 (q, *J* 8.0 Hz, 2H, H-12), 3.45 (m, 2H, H-6), 2.87 (t, *J* 5.0 Hz, 2H, H-5), 1.84 (s, 3H, H-14), 1.27 (t, *J* 8.0 Hz, 3H, H-13); ^{13}C NMR (100 MHz, $CDCl_3$) δ 170.6 (C-10), 161.6 (C-8), 138.6 (C-4), 128.8 (C-2), 128.6 (C-3), 126.6 (C-1), 82.3 (C-9), 58.3 (C-12), 44.8 (C-6), 37.3 (C-5), 19.3 (C-14), 14.7 (C-13).

Ethyl-(2*Z*)-3-{[2-(4-methoxyphenyl)ethyl]amino}but-2-enoate (EN2)

Light yellow oil; n_p^a = 1.551; ^{1}H NMR (500 MHz, $CDCl_3$) δ 8.65 (s, 1H, H-7), 7.14 (d, 2H, *J* 9.0 Hz, H-2), 6.87 (d, 2H, *J* 8.0 Hz, H-3), 4.44 (s, 1H, H-9), 4.11 (q, *J* 8.0 Hz, 2H, H-12), 3.80 (s, 3H, H-15), 3.43 (m, 2H, H-6), 2.80 (t, *J* 5.0 Hz, 2H, H-5), 2.27 (s, 3H, H-14), 1.27 (t, *J* 8.0 Hz, 3H, H-13); ^{13}C NMR (100 MHz, $CDCl_3$) δ 170.6 (C-10), 161.7 (C-8), 158.3 (C-1), 130.6 (C-3), 129.7 (C-4), 114.0 (C-2), 82.2 (C-9), 58.3 (C12), 55.2 (C-15), 45.0 (C-6), 36.4 (C-5), 19.3 (C-14), 14.7 (C-13).

Electrochemical measurements

Solution preparation

The solutions of EN1 and EN2 were prepared in concentrations of 1.0×10^{-2}, 1.0×10^{-3}, 1.0×10^{-4} and 1.0×10^{-5} mol L^{-1} in aqueous solution of 0.5 mol L^{-1} HCl

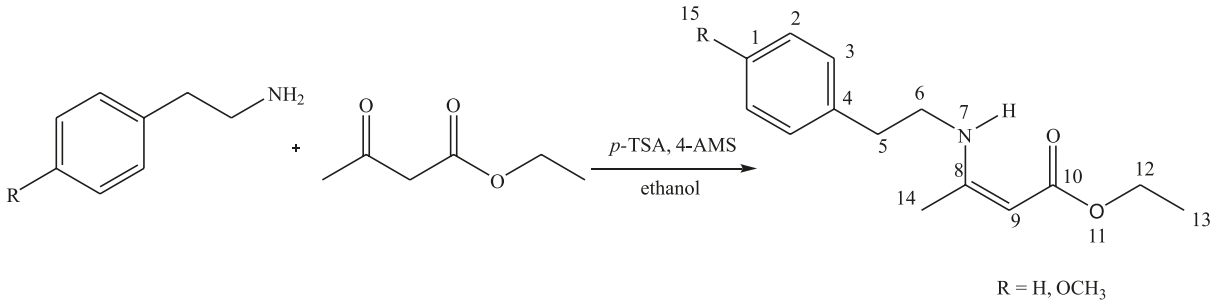

Figure 1. Synthetic route of the β-enaminoesters studied.

and 45% of ethanol for complete solubilization, because these compounds were not completely soluble in water.

Electrochemical tests

The assays were tested at 30 °C using the electrochemical cell of three electrodes: carbon steel with 0.80 cm^2 of area, a platinum electrode as the auxiliary electrode and silver-silver chloride (Ag/AgCl, 3.0 mol L^{-1} KCl) as a reference electrode.

Before each experiment, the work electrode was abraded with 400, 600, and 1200-grade emery paper, washed with distilled water, degreased with ethanol and dried. The tests were carried out in aerated media using the Autolab Potentiostat/Galvanostat model PGSTAT 302N and analyzed with NOVA 1.11 software.

EIS

The open circuit potential (OCP) was monitored before each assay for 30 min until a stabilized potential was observed.[14,15] After that, impedance measurements were taken at a frequency interval of 10 kHz to 0.1 Hz with 10 mV of amplitude peak-by-peak. The inhibition efficiency (η) was calculated using equation 1:[2,3,16,17]

$$\eta_{EIS}(\%) = \frac{R_{ct} - R^0_{ct}}{R_{ct}} \times 100 \quad (1)$$

where R_{ct} is the charge transfer resistance in the presence of the inhibitor, and R^0_{ct} is the charge transfer resistance in the absence of the inhibitor.[18] All values were obtained from the Nyquist diagram of each experiment.[19]

LPR

LPR tests were performed using a scan rate of 1 mV s^{-1} in the potential range of ± 10 mV around the open circuit potential (E_{OCP}).[20] The inhibition efficiency was calculated using equation 2:

$$\eta_{LPR}(\%) = \frac{R_p - R^0_p}{R_p} \times 100 \quad (2)$$

where R_p is resistance of polarization in the presence of the inhibitor, and R^0_p is the resistance in the absence of the inhibitor. The values of R_p are the values of the angular coefficient obtained by a linear regression of the graph of current density (i) *vs.* potential (E).

PP

PP tests were performed using a scan rate of 1 mV s^{-1} in the potential range of ± 200 mV around E_{OCP}. Inhibition efficiency was calculated using equation 3:[2,3,21]

$$\eta_{PP}(\%) = \frac{i_{corr,0} - i_{corr}}{i_{corr,0}} \times 100 \quad (3)$$

where $i_{corr,0}$ and i_{corr} are the uninhibited and the inhibited corrosion current densities, respectively.

Weight loss experiment (WL)

The gravimetric measurements were taken using samples of AISI 1020 carbon steel of 3.0 × 3.0 × 0.1 cm in a solution of 0.5 mol L^{-1} HCl in the presence and absence of EN1 in a concentration of 1.0×10^{-2} mol L^{-1} for 3, 6, 18 and 24 h.[22] The experiments were conducted in triplicate. The samples were abraded with 400, 600, and 1200-grade emery paper, washed with distilled water, degreased with ethanol and dried.

The assays were tested with the samples of carbon steel immersed in a corrosive medium in the presence and absence of an inhibitor at 30 °C and in naturally aerated media for 3, 6, 18 and 24 h.[13,23] The inhibition efficiency was calculated using equation 4:

$$\eta_{WL}(\%) = \frac{W_0 - W}{W_0} \times 100 \quad (4)$$

where W_0 and W are the weight loss in the absence and presence of the studied inhibitors, respectively.

Surface analysis

SEM

The samples of carbon steel of 3.0 × 3.0 × 0.1 cm were abraded and washed with ethanol, dried and immersed in the presence or absence of the inhibitor and in the presence of 0.5 mol L^{-1} HCl for 24 h at room temperature. The specimens were removed, washed with water and ethanol, and dried. The measurements were taken using a Hitachi TM 3000 tabletop microscope.[24]

Results and Discussion

Synthesis

EN1 and EN2 were obtained in good yields of 74 and 80%, respectively, by synthetic routes adapted from the literature.[25,26] The products were isolated in oil form. The characterizations were determined by ^{13}C and ^{1}H NMR spectroscopy and compared with the reported data.[26]

EIS

The corrosion behavior of AISI 1020 carbon steel in 0.5 mol L^{-1} HCl solution obtained in the presence and absence of the β-enaminoesters was investigated by EIS at 30 °C after 30 min of immersion, when the stabilization of the OCP was observed. The Nyquist plots obtained by EIS measurements in the absence and presence of EN1 and EN2 are shown in Figure 2.

The diameter of the semicircular Nyquist plots, in both cases, increases with an increment in the concentration of

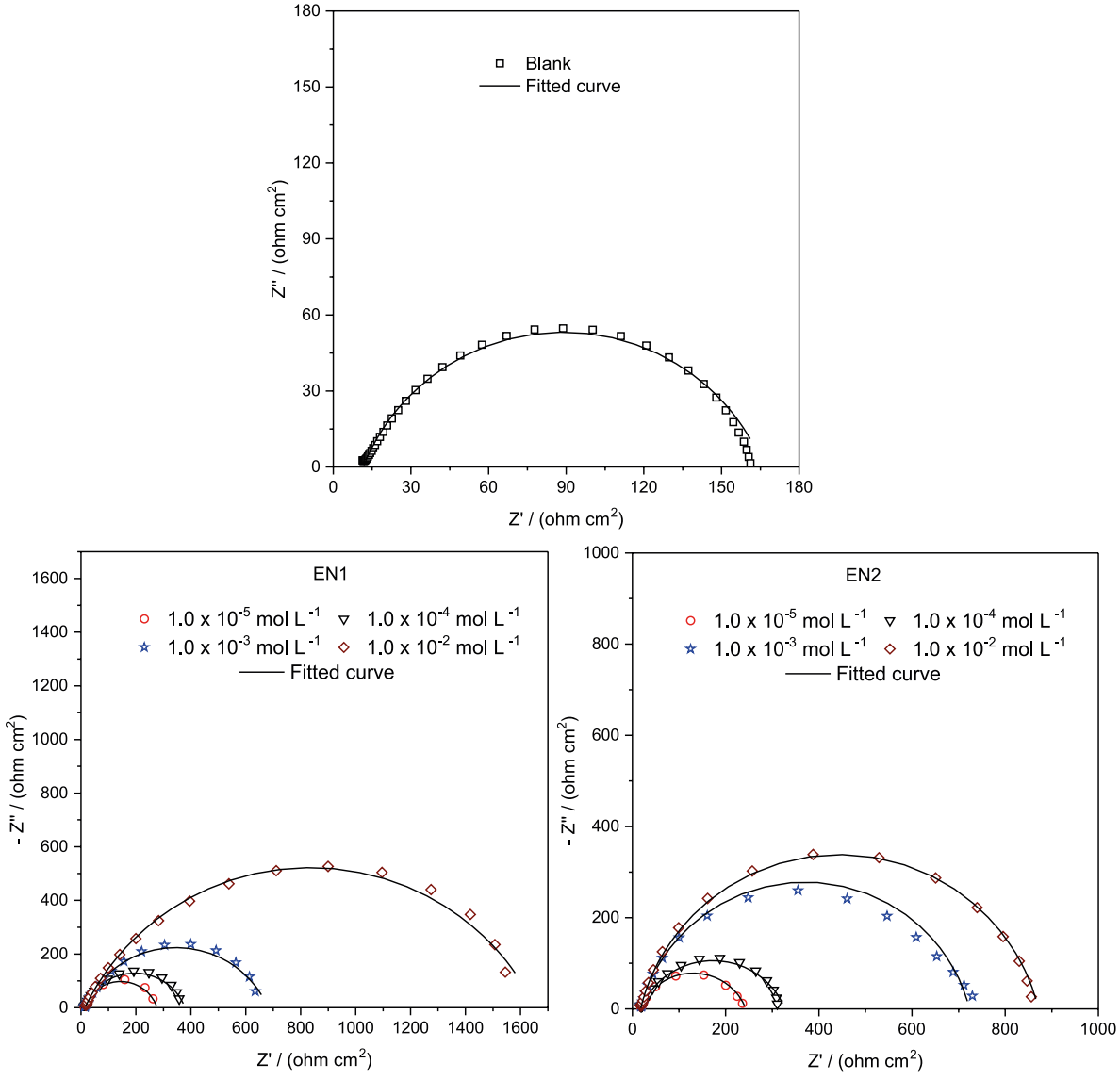

Figure 2. Nyquist plots obtained in absence and presence of EN1 and EN2, against AISI 1020 carbon steel in 0.5 mol L^{-1} HCl.

the inhibitors, showing that the corrosion and inhibition processes are charge-transfer-controlled. The charge transfer resistance values (R_{ct}) were obtained by Z' in the x-axis, where the intersection at high frequency is the ohmic resistance of the solution (R_s), and the intersection at low frequency is the $R_{ct} + R_s$. Thus, the R_{ct} values were calculated by the difference between ($R_{ct} + R_s$) and R_s.

The degree of surface coverage (θ) is proportional to the inhibition corrosion efficiency and this may be calculated by equation 5:

$$\theta = \frac{R_{ct} - R^0_{ct}}{R_{ct}} \quad (5)$$

where R_{ct} and R^0_{ct} are the charge transfer resistances in the presence and absence of the inhibitor, respectively, as obtained by EIS.

For the investigation of impedance plots containing a capacitive semi-circle, the [R(RQ)] circuit was used as shown in Figure 3.[23]

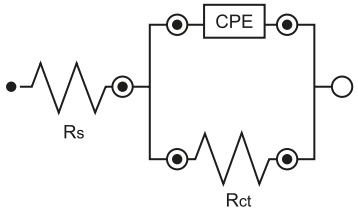

Figure 3. Equivalent circuit used to fit the impedance spectra in the absence and presence of the inhibitors EN1 and EN2.

According to results, the EIS data are analyzed using the [R(RQ)] equivalent circuit (Figure 3) that includes the solution resistance (R_s), polarization resistance (R_p) and constant phase element (CPE), which can be represented in equation 6:[23]

$$Z_{CPE} = Y_0^{-1} (jw)^{-n} \quad (6)$$

where Y_0 is the magnitude of the CPE, n is the phase shift, j is the imaginary unit and w is the angular frequency. CPE is introduced in the circuit instead of a pure double layer capacitor to give a more accurate fit.[20-23]

The double layer capacitances (C_{dl}) for a circuit including a CPE were calculated from the following equation 7:[21-23]

$$C_{dl} = Y_0 (2\pi f_{max})^{n-1} \quad (7)$$

where f_{max} is the frequency at which the imaginary component of the impedance is maximal. The parameters obtained by EIS can be observed in Table 1.

The R_{ct} values observed for EN1 were better than those observed for EN2. Consequently, EN1 is more efficient as an inhibitor than EN2, as shown in Table 1. This increase of R_{ct} values with an increment in the concentration of EN1 and EN2 can be attributed to an increase in the surface coverage on the metal surface by molecules of the β-enaminoester.

The decreased values of C_{dl} indicates a decrease in the local dielectric constant, suggesting that the inhibitor molecules act by adsorbing on the metal/solution interface.

The Bode plots of the evaluated compounds are shown in Figure 4. An increase in the Z_{mod} when the concentration of EN1 and EN2 increases indicates better performance.[27] Adsorption of the EN1 and EN2 on the metal surface lowered the surface heterogeneities, and as a result, the phase angle increased, approaching 90°.[17,28,29]

LPR

The LPR measurements were performed after the

Table 1. Impedance parameters for AISI 1020 carbon steel in 0.5 mol L^{-1} HCl solution in the absence and presence of EN1 and EN2

Inhibitor	C_{inh}[a] / (mol L^{-1})	OCP[b] *vs.* Ag/AgCl / mV	R_{ct}[c] / (Ω cm^2)	n[d]	Y_0[e] / (μOhm cm^{-2})	f_{max}[f] / Hz	C_{dl}[g] / (μF cm^{-2})	θ[h]	η_{EIS}[i] / %
Blank	–	–461	149.83	0.767	205	8.68	80.75	–	–
EN1	1.0×10^{-5}	–454	251.81	0.810	154	5.42	78.78	0.404	40
	1.0×10^{-4}	–456	344.69	0.784	143	5.42	72.38	0.565	56
	1.0×10^{-3}	–442	621.84	0.750	141	3.39	74.91	0.759	76
	1.0×10^{-2}	–409	1512.83	0.722	65	2.12	36.49	0.901	90
EN2	1.0×10^{-5}	–500	228.36	0.774	182	8.68	73.72	0.344	34
	1.0×10^{-4}	–481	293.36	0.763	156	6.86	63.94	0.489	49
	1.0×10^{-3}	–470	721.16	0.850	42	8.68	23.05	0.792	79
	1.0×10^{-2}	–472	840.23	0.853	37	6.86	21.33	0.821	82

[a]Inhibitor concentration; [b]open circuit potential; [c]resistance of charge transference; [d]phase shift; [e]magnitude of constant phase element (CPE); [f]frequency of maximal impedance; [g]double layer capacitance; [h]degree of surface coverage; [i]inhibition efficiency obtained by electrochemical impedance spectroscopy. EN1: ethyl-(2*Z*)-3-[(2-phenylethyl)amino]but-2-enoate; EN2: ethyl-(2*Z*)-3-{[2-(4-methoxyphenyl)ethyl]amino}but-2-enoate.

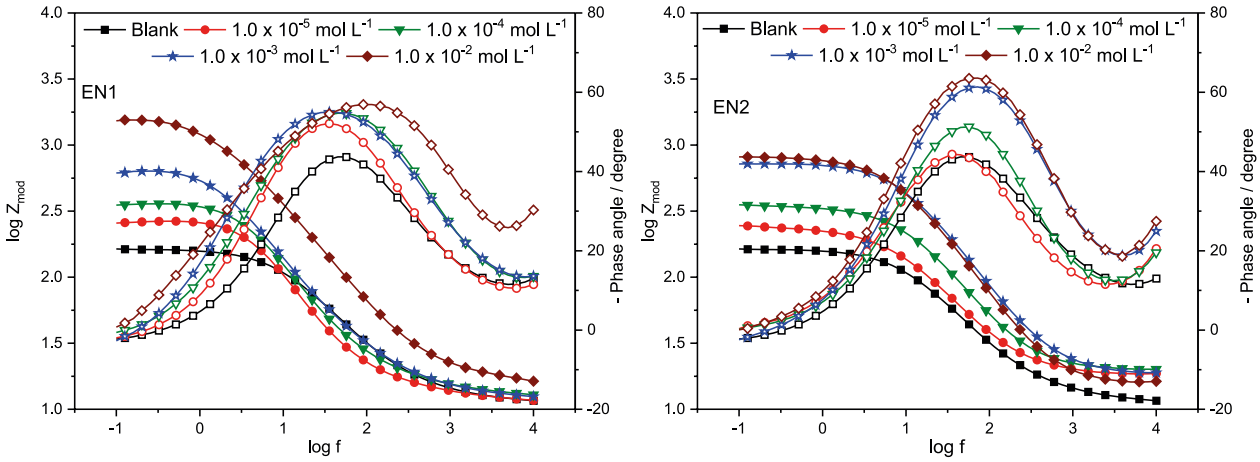

Figure 4. Bode impedance plots for the carbon steel obtained in 0.5 mol L^{-1} HCl in the presence and absence of EN1 and EN2.

EIS assays in the presence and absence of the inhibitors using AISI 1020 carbon steel against 0.5 mol L^{-1} HCl. The obtained data were submitted to the linear regression, and the efficiency values were calculated by equation 2, using the R_p values (angular coefficient). The results of corrosion inhibition efficiency obtained by the LPR measurements corroborated the results observed in the EIS assays, where EN1 presented a better performance in the studied concentrations. The R_p values and inhibition efficiency values are shown in Table 2.[2]

Table 2. LPR parameters for AISI 1020 carbon steel in 0.5 mol L^{-1} HCl solution in the absence and presence of EN1 and EN2

Inhibitor	C_{inh}[a] / (mol L^{-1})	r[b]	R_p[c] / (Ω cm^2)	θ[d]	η_{LPR}[e] / %
Blank	–	0.9599	180.22	–	–
EN1	1.0×10^{-5}	0.9791	268.31	0.3283	33
	1.0×10^{-4}	0.9376	358.01	0.4966	50
	1.0×10^{-3}	0.9286	598.67	0.6990	70
	1.0×10^{-2}	0.9401	2208.86	0.9184	92
EN2	1.0×10^{-5}	0.9034	447.25	0.4963	49
	1.0×10^{-4}	0.9313	483.13	0.5337	53
	1.0×10^{-3}	0.8974	805.41	0.7203	72
	1.0×10^{-2}	0.8109	1175.90	0.8084	81

[a]Inhibitor concentration; [b]coefficient of correlation; [c]resistance of polarization; [d]degree of surface coverage; [e]inhibition efficiency obtained by the linear polarization resistance measurements. EN1: ethyl-(2*Z*)-3-[(2-phenylethyl) amino]but-2-enoate; EN2: ethyl-(2*Z*)-3-{[2-(4-methoxyphenyl)ethyl]amino} but-2-enoate.

Both studied molecules (EN1 and EN2) presented the same basic structure, where the adsorption on the metallic surface occurs through the enamino portion, but the corrosion inhibition efficiencies observed are different for the two structures. This fact can be associated with the methoxy group being present in EN2; this group contains an oxygen atom that can form the hydrogen bond with water molecules, thus approaching the water molecules on the metal surface, increasing the corrosive process.

PP

The experiments were conducted after the LPR measurement at room temperature (25 °C) in 0.5 mol L^{-1} HCl in the presence and absence of inhibitors. By using the PP technique, it was possible to obtain the current density illustrated by Tafel plots.[3,14] In Figure 5, it is possible to observe the polarization curves obtained in the presence and absence of EN1 and EN2.

Table 3 presents the electrochemical parameters obtained by Tafel extrapolation and the corrosion inhibition efficiency.

According to the polarization curves (Figure 5) and Table 3, the presence of inhibitors promotes a decrease in the current densities in cathodic and anodic branches and a slight shift of E_{corr} in the anodic direction. This fact indicates that EN1 and EN2 acted as mixed-type corrosion inhibitors that could retard both metal dissolution and the cathodic process.[3,14,16,23,30]

Thus, when the corrosion inhibition efficiencies for EN1, at the concentration of 1.0×10^{-2} mol L^{-1}, were compared using the PP, LPR and EIS techniques, the obtained values, 89, 92 and 90%, respectively, indicated a good correlation.

WL

Immersion time

The gravimetric assay was performed only for the inhibitor that showed better efficiency, EN1, in 1.0×10^{-2} mol L^{-1}. The weight loss of AISI 1020 carbon steel was determined at 30 °C after 3, 6, 18, and 24 h of

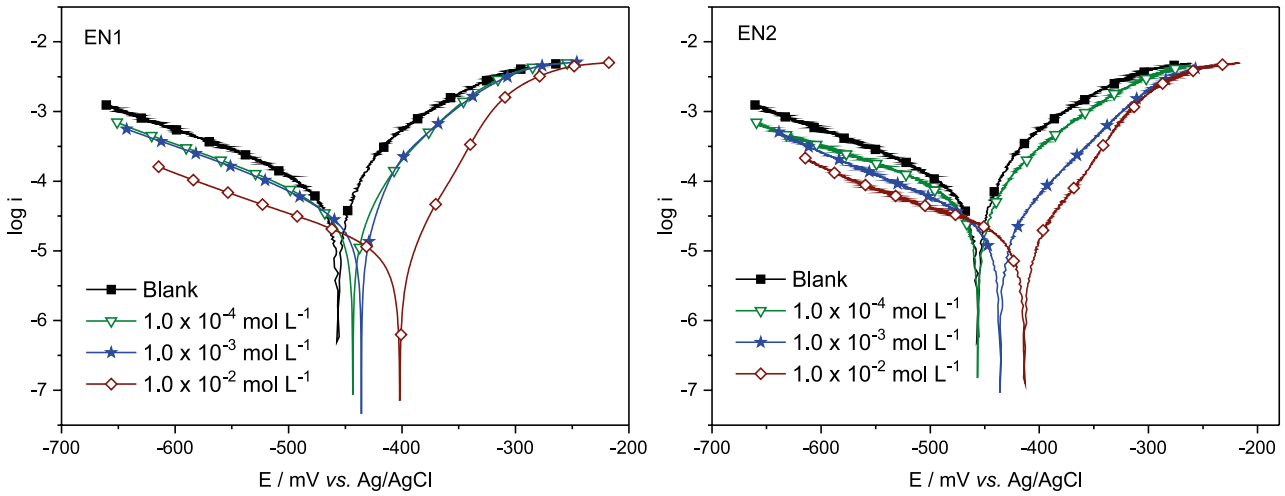

Figure 5. Polarization curves of carbon steel in 0.5 mol L^{-1} HCl in the presence and absence of EN1 and EN2.

Table 3. Electrochemical parameters from carbon steel obtained by potentiodynamic polarization measurements in the presence and absence of EN1 and EN2 in 0.5 mol L^{-1} HCl

Inhibitor	C_{inh}[a] / (mol L^{-1})	E_{corr}[b] / mV *vs.* Ag/AgCl	j_{corr}[c] / (mA cm^{-2})	β_a[d] /(mV dec^{-1})	$-\beta_c$[e] /(mV dec^{-1})	θ[f]	η_{PP}[g] / %
Blank	–	–458	75.7	165.4	61.4	–	–
EN1	1.0×10^{-4}	–443	33.2	146.4	53.9	0.561	56
	1.0×10^{-3}	–435	21.0	119.7	33.9	0.722	72
	1.0×10^{-2}	–402	8.0	144.1	39.2	0.894	89
EN2	1.0×10^{-4}	–465	63.5	178.6	66.7	0.161	16
	1.0×10^{-3}	–465	28.1	191.9	64.8	0.628	63
	1.0×10^{-2}	–457	27.3	178.6	65.3	0.639	64

[a]Inhibitor concentration; [b]corrosion potential; [c]corrosion current density; [d]anodic Tafel slope; [e]cathodic Tafel slope; [f]degree of surface coverage; [g]inhibition efficiency obtained by potentiodynamic polarization measurements. EN1: ethyl-(2*Z*)-3-[(2-phenylethyl)amino]but-2-enoate; EN2: ethyl-(2*Z*)-3-{[2-(4-methoxyphenyl)ethyl]amino}but-2-enoate.

immersion in 0.5 mol L^{-1} HCl in the presence and absence of the inhibitor. The corrosion rates and the inhibition efficiency were calculated from the mass loss data, and the results are shown in Table 4.[31,32]

In Table 4, it is possible to observe the increase of the corrosion efficiency inhibition with the increase of the immersion time. This behavior can be attributed to the interaction of the inhibitor molecules with the metal surface across the formation of a stable and passive film. The lone electron pairs of nitrogen and oxygen atoms, and the π electrons of β-enamine conjugated double bond may be involved in this interaction. The better inhibition efficiency (98%) was observed after 24 h of immersion, which indicated that the inhibition efficiency remains high long after the treatment, and the compound stability in HCl solution is good when compared with other analogous compounds.[33-35]

Table 4. Weight loss data for AISI 1020 carbon steel in 0.5 mol L^{-1} HCl solution in the absence and presence of EN1 at 30 °C

time / h	Blank	EN1	
	W_{corr}[a] / (g cm^{-2} h^{-1})	W_{corr}[b] / (g cm^{-2} h^{-1})	η[c] / %
3	1.90×10^{-4}	2.02×10^{-5}	89
6	4.14×10^{-4}	4.21×10^{-5}	90
18	8.82×10^{-4}	4.38×10^{-5}	95
24	2.45×10^{-3}	4.71×10^{-5}	98

[a]Weight loss in the absence of inhibitor; [b]weight loss in the presence of EN1; [c]inhibition efficiency. EN1: ethyl-(2*Z*)-3-[(2-phenylethyl)amino]but-2-enoate.

The corrosion inhibition efficiency observed for the gravimetric method, 89% after 3 h of immersion time, was similar to the obtained values by electrochemical methods (89, 92 and 90% by PP, LPR and EIS, respectively), for EN1 at the same concentration, showing, thus, a good correlation.

Effect of temperature

The working temperature can influence the corrosion inhibition efficiency, and generally the corrosion rate

increases with an increase of the temperature; this fact is due to the accelerated evolution of H_2 and, consequently, higher dissolution of the metal.[36]

Therefore, the effect of temperature was analyzed at 303, 313, 323, and 333 K, only for the inhibitor that showed better efficiency, EN1, at 1.0×10^{-2} mol L^{-1} during 3 h of immersion in the presence of 0.5 mol L^{-1} HCl solution. The inhibition efficiencies (η (%)) at different temperatures can be seen in Table 5.

Table 5. Weight loss data for AISI 1020 carbon steel in 0.5 mol L^{-1} HCl solution in the absence and presence of EN1 at 303, 313, 323, 333 K

Temperature / K	Blank	EN1	
	W_{corr} [a] / (g cm^{-2} h^{-1})	W_{corr} [b] / (g cm^{-2} h^{-1})	η[c] / %
303	1.4×10^{-4}	2.0×10^{-5}	89
313	5.2×10^{-4}	5.9×10^{-5}	89
323	9.6×10^{-4}	1.0×10^{-4}	89
333	16.6×10^{-4}	2.3×10^{-4}	86

[a]Weight loss in the absence of inhibitor; [b]weight loss in the presence of EN1; [c]inhibition efficiency. EN1: ethyl-(2*Z*)-3-[(2-phenylethyl)amino] but-2-enoate.

Stability in the efficiency of inhibition of EN1 was observed in temperatures of 303, 313, and 323 K, characterizing this compound as an efficient and stable corrosion inhibitor for AISI 1020 carbon steel, in 0.5 mol L^{-1} HCl solution, at different temperatures. One decrease of only 3% of the inhibition efficiency was observed at 333 K.

The energy barrier for the corrosion reaction is an important thermodynamic parameter that should be observed when studying corrosion inhibitors and can be calculated using the temperature variation. This energy value is represented by the apparent activation energy (E_a). In this work, the E_a was calculated for AISI 1020 carbon steel corrosion in the presence and absence of EN1 in acid solution, using an Arrhenius plot in accordance with equation 8:[36,37]

$$\ln W_{corr} = \frac{-E_a}{RT} + \ln A \quad (8)$$

where $\ln W_{corr}$ is the corrosion rate, E_a is the apparent activation energy, A is the frequency factor, T is the absolute temperature and R is the molar gas constant. Arrhenius plots of $\ln W_{corr}$ *vs.* 1 / T with and without EN1 are shown in Figure 6.[37-39]

Table 6 shows the correlation coefficient obtained with a linear regression of the Arrhenius plot ($\ln W_{corr}$ *vs.* 1 / T) and the E_a obtained according to equation 6, both in the presence and absence of an inhibitor.

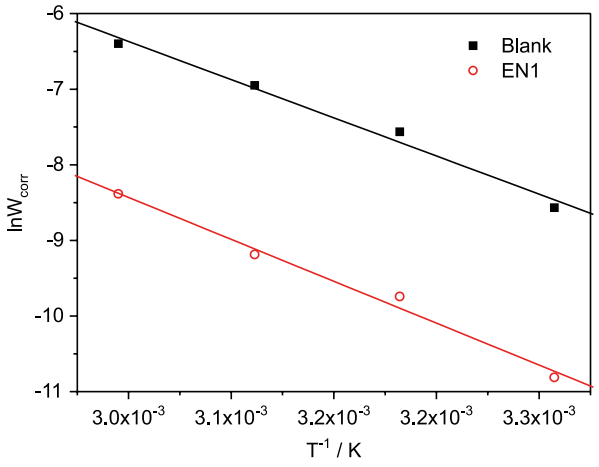

Figure 6. Arrhenius plots in carbon steel in 0.5 mol L^{-1} HCl solution in the absence (blank) and presence of EN1 (1.0×10^{-2} mol L^{-1}).

Table 6. Linear regression parameters obtained from Arrhenius plots

Compound	Concentration / (mol L^{-1})	E_a [a] / (mol L^{-1})	Correlation coefficient (r)
Blank	–	60.02	0.9925
EN1	1.0×10^{-2}	65.91	0.9942

[a]Apparent activation energy. EN1: ethyl-(2*Z*)-3-[(2-phenylethyl)amino] but-2-enoate.

As observed in Table 6, the E_a is higher in the presence of EN1 when compared with that of the blank solution. This fact is due to the increased thickness of the double layer, which enhances the activation energy of the corrosion process, requiring a higher energy for the corrosion reaction to occur.[39-41]

Adsorption isotherm

The efficiency of an organic inhibitor relies on its ability to be adsorbed onto the metal surface. The interaction between the inhibitor and the metal surface can be evaluated by adsorption isotherms.[42]

In the present work, attempts were made to fit these values as a function of concentration of EN1 and EN2, employing three isotherms, including Langmuir, Temkin and Frumkin, and the correlation coefficients were evaluated to choose the more adjusted model.[38] The corresponding mathematical equations are shown below, and Figure 7 shows the application of the three isotherm models to the study of the adsorption of β-enaminoesters on the carbon steel surface.

$$\text{Langmuir: } \frac{C}{\theta} = \frac{1}{K_{ads}} + C \quad (9)$$

$$\text{Temkin: } \theta = -\frac{\ln K_{ads}}{2a} - \frac{\ln C}{2a} \quad (10)$$

$$\text{Frumkin: } \frac{\ln\theta}{(1-\theta)} = \ln K_{ads} + 2a\theta \quad (11)$$

where C is the inhibitor concentration, K_{ads} is the equilibrium constant of the adsorption process, θ is the degree of surface coverage, and a is the interaction parameter.

Table 7 shows the values of the parameters of the linearized Langmuir, Temkin and Frumkin adsorption isotherms for EN1 and EN2.

Table 7 shows the correlation coefficient values of three adsorption isotherm models and their slopes. Better correlation coefficients for both compounds (EN1 and EN2) were obtained by the Langmuir isotherm. However, the slope observed for the studied compounds differed by approximately 0.1, as expected from the Langmuir adsorption model, suggesting that each molecule of EN1 and EN2 occupies approximately 1.09 and 1.22 adsorption sites of the metal surface, respectively. Thus, a modified Langmuir adsorption isotherm was chosen in accordance with the literature, which is given by equation 12.[38-41,43-47]

Table 7. Values of parameters of linearized Langmuir, Temkin and Frumkin adsorption isotherms for EN1 and EN2 on AISI 1020 carbon steel in 0.5 mol L^{-1} HCl

Adsorption isotherm	Inhibitor	Correlation coefficient (r)	Slope
Langmuir	EN1	0.9998	1.09
	EN2	0.9999	1.22
Temkin	EN1	0.9990	0.07
	EN2	0.9712	0.09
Frumkin	EN1	0.9940	–9.06
	EN2	0.9209	–5.75

EN1: ethyl-(2*Z*)-3-[(2-phenylethyl)amino]but-2-enoate; EN2: ethyl-(2*Z*)-3-{[2-(4-methoxyphenyl)ethyl]amino}but-2-enoate.

$$\frac{C}{\theta} = \frac{n}{K_{ads}} + nC \quad (12)$$

where n is a correction parameter of slope. The linear coefficient allowed the evaluation of K_{ads} and the free energy of adsorption (ΔG^0_{ads}) calculated by equation 13.

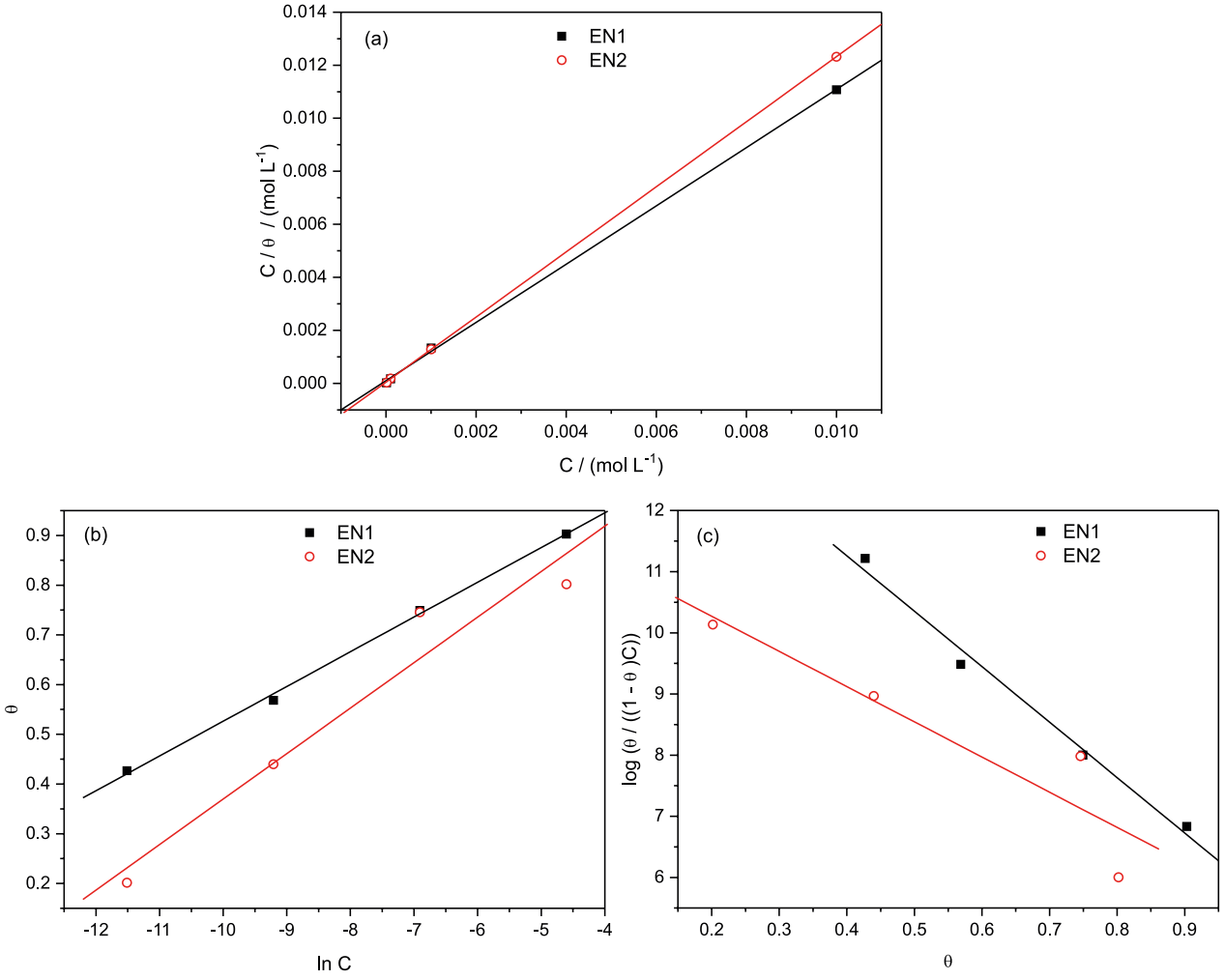

Figure 7. (a) Langmuir isotherm, (b) Temkin isotherm, and (c) Frumkin isotherm for EN1 and EN2 on carbon steel in 0.5 mol L^{-1} HCl.

$$\Delta G^{0}_{ads} = -RT\ln(55.55)K_{ads} \quad (13)$$

where R is the universal gas constant (J K^{-1} mol^{-1}), T is the temperature (K), and 55.55 is the molar concentration (mol L^{-1}) of water in the solution.

The K_{ads} and ΔG^{0}_{ads} values and the modified adsorption Langmuir isotherm parameters are shown in Table 8.

Table 8. Thermodynamic parameters for the adsorption of EN1 and EN2 in 0.5 mol L^{-1} HCl on AISI 1020 carbon steel

Inhibitor	Slope	n[a]	K_{ads}[b] / (L mol^{-1})	ΔG^{0}_{ads}[c] / (kJ mol^{-1})
EN1	1.09	0.92	9.16×10^{3}	–32.55
EN2	1.22	0.82	17.70×10^{3}	–34.18

[a]Correction parameter of slope; [b]adsorption constant; [c]free energy of adsorption. EN1: ethyl-(2*Z*)-3-[(2-phenylethyl)amino]but-2-enoate; EN2: ethyl-(2*Z*)-3-{[2-(4-methoxyphenyl)ethyl]amino}but-2-enoate.

The high values of K_{ads} are indicative of a high adsorption percentage of inhibitor molecules on the metal surface, and the negative values of ΔG^{0}_{ads} indicate a higher spontaneous corrosion inhibition process for these compounds.[46] The ΔG^{0}_{ads} values vary from –34.18 to –32.55 kJ mol^{-1}, indicating that EN1 and EN2 adsorbed onto carbon steel surface via mixed mechanisms.[48,49]

SEM

The SEM images of inhibited (EN1) and uninhibited (blank) AISI 1020 carbon steel coupons after immersion in 0.5 mol L^{-1} HCl for 24 h are shown in Figure 8. The SEM image of the blank, in the absence of an inhibitor, is highly damaged; however, in the presence of EN1, the surface is smoother.

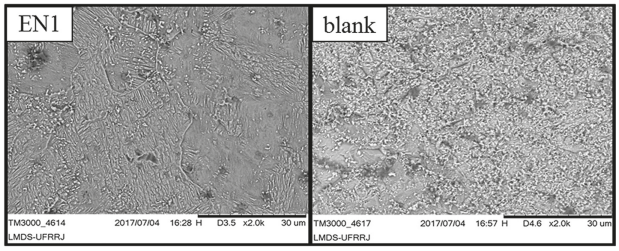

Figure 8. SEM micrograph (2000 ×) of AISI 1020 carbon steel immersed in 0.5 mol L^{-1} HCl in the presence (EN1) and absence (blank) of inhibitor.

Further, the image of carbon steel in the absence of an inhibitor (blank) indicated the presence of white flakes, which could be due to oxidation products that form as result of corrosion processes on the metal surface.[15,50] When EN1 was utilized, the presence of flakes was minimized, and it is possible to observe the grooves caused by using emery paper after the preparation of the metallic surface, confirming that EN1 acts as an efficient inhibitor of corrosion because the metal surface was preserved.

Inhibition mechanism

Metallic corrosion is a consequence of the formation of an electric double layer on the metal surface caused by water molecules and chloride ions when in HCl medium. The use of the corrosion inhibitor is very important due to the interaction of the inhibitor/surface, which results in the formation of a protective layer that decreases the double layer, thus retarding the corrosive process. The adsorption process can be physical or chemical, in accordance with the inhibitor structure. Inhibitors that contain heteroatoms are absorbed by chemisorption, donating electrons to metal, but compounds that have π bonds and/or its heteroatoms protonated are adsorbed by physisorption.[22,51]

Figure 9 illustrates a corrosive medium in the absence and presence of an inhibitor. It can be observed that in the absence of an inhibitor flawed regions are formed because of the attachment by chloride and hydronium ions. After an ideal concentration of an inhibitor is added, the inhibitor molecules form a protective barrier that prevents the approach of corrosive particles, such as chloride and hydronium ions, thus preserving the metal surface.[22,51]

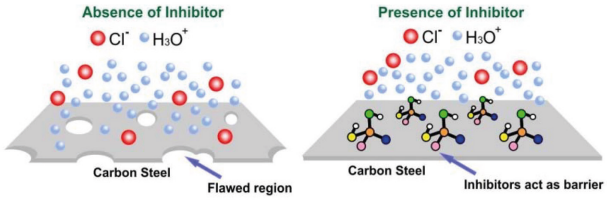

Figure 9. Illustration of corrosive mechanism.

Conclusions

Both the inhibitors showed a good efficiency of anticorrosive action for AISI 1020 carbon steel in 0.5 mol L^{-1} HCl, and their efficiency increased with concentration. The best inhibitor was EN1 at a concentration of 1.0×10^{-2} mol L^{-1}. Good correlations were observed between the results obtained for PP, LPR, EIS and WL. The results obtained from the polarization curves suggested that EN1 and EN2 act as mixed inhibitors that reduce both the anodic and cathodic current densities. The maximum corrosion inhibitor efficiency for EN1 (1.0×10^{-2} mol L^{-1}) was 98%, observed after 24 h of immersion in the presence of 0.5 mol L^{-1} HCl. The surface coverage obtained from the EIS measurements fits well with the modified Langmuir

adsorption isotherm, with correlation coefficients and slopes near unity. The SEM analysis showed that the metal surface was protected by the use of EN1 as a corrosion inhibitor.

Acknowledgments

The authors are very grateful to Coordenação de Aperfeiçoamento de Pessoal de Nível Superior (CAPES), Conselho Nacional de Desenvolvimento Científico e Tecnológico (CNPq), Fundação de Amparo à Pesquisa do Estado do Rio de Janeiro (FAPERJ) and Petróleo Brasileiro S. A. (Petrobras), as well as to the P&D ANEEL-SUPERCABO project for financial support.

References

1. Li, X.; Deng, S.; Fu, H.; *Corros. Sci*. **2010**, *52*, 3413.
2. Valbon, A.; Neves, M. A.; Echevarria, A.; *Int. J. Electrochem. Sci.* **2017**, *12*, 3072.
3. Goulart, C. M.; Esteves-Souza, A.; Martinez-Huitle, C. A.; Rodrigues, C. J. F.; Maciel, M. A. M.; Echevarria, A.; *Corros. Sci*. **2013**, *67*, 281.
4. Safak, S.; Duran, B.; Yurt, A.; Tukoglu, G.; *Corros. Sci*. **2012**, *54*, 251.
5. Obot, I. B.; Obi-Egbedi, N. O.; *Corros. Sci.* **2010**, *52*, 198.
6. Abdul, A. S. N.; Hussain, A. A.; *J. Basrah Res.* **2012**, *38*, 125.
7. Ferraz, H. M. C.; Pereira, L. C.; *Quim. Nova* **2004**, *27*, 89.
8. Gholap, A. R.; Chakor, N. S.; Daniel, T.; Lahoti, R. J.; Srinivasan, K. V.; *J. Mol. Catal. A: Chem.* **2006**, *245*, 37.
9. Morales-Rios, M. S.; Suarez-Castillo, O. R.; Alvarez-Cisneros, C.; Joseph-Nathan, P.; *Can. J. Chem.* **1999**, *77*, 130.
10. Prajila, M.; Abraham, J.; *J. Mol. Liq.* **2017**, *241*, 1.
11. Heydari, H.; Talebian, M.; Salarvand, Z.; Raeissi, K.; Bagheri, M.; Golozar, M. A.; *J. Mol. Liq.* **2018**, *254*, 177.
12. Laskar, R. A.; Begum, N. A.; Mir, M. H.; Ali, S.; Khan, A. T.; *Tetrahedron Lett.* **2013**, *54*, 436.
13. Al-Matar, H. M.; Khalil, K. D.; Al-Kanderi, M. F.; Elnagdi, M. H.; *Molecules* **2012**, *17*, 897.
14. Singh, P.; Quraishi, M. A.; *Measurement* **2016**, *86*, 114.
15. Yurt, A.; Duran, B.; Dal, H.; *Arabian J. Chem.* **2014**, *7*, 732.
16. Albuquerque, M. A.; Oliveira, M. C. C.; Echevarria, A.; *Int. J. Electrochem. Sci.* **2017**, *12*, 852.
17. Chaitra, T. K.; Mohana, K. N. S.; Tandon, H. C.; *J. Mol. Liq.* **2015**, *211*, 1026.
18. Gupta, S. R.; Mourya, P.; Singh, M. M.; Singh, V. P.; *J. Organomet. Chem.* **2014**, *767*, 136.
19. Kumar, C. B. P.; Mohana, K. N.; *J. Taiwan Inst. Chem. Eng.* **2014**, *45*, 1031.
20. Ituen, E.; James, A.; Akaranta, O.; Sun, S.; *Chin. J. Chem. Eng.* **2016**, *24*, 1442.
21. Mendonça, G. L. F.; Costa, S. N.; Freire, V. N.; Cascianoa, P. N. S.; Correia, A. N.; Lima-Neto, P.; *Corros. Sci.* **2017**, *115*, 41.
22. Khan, G.; Basirun, W. J.; Kazi, S. N.; Ahmed, P.; Magaji, L.; Ahmed, S. M.; Khan, G. M.; Rehman, M. A.; *J. Colloid Interface Sci.* **2017**, *502*, 134.
23. Torres, V. V.; Rayol, V. A.; Magalhães, M.; Viana, G. M.; Aguiar, L. C. S.; Machado, S. P.; Orofino, H.; D'Elia, E.; *Corros. Sci.* **2014**, *79*, 108.
24. Sukach, V. A.; Tkachuck, V. M.; Rusanov, E. B.; Roschenthaler, G. V.; Vovk, M. V.; *Tetrahedron* **2012**, *68*, 8408.
25. Kalshetty, B. M.; Gani, R. S.; Chandrasekhar, V. M.; Kalashetti, M. B.; *J. Chem., Biol. Phys. Sci.* **2012**, *2*, 1736.
26. Singh, A.; Gupta, N.; Sharma, M. L.; Singh, J.; *Indian J. Chem., Sect. B: Org. Chem. Incl. Med. Chem.* **2014**, *53*, 900.
27. Abd El-Lateef, H. M.; *Corros. Sci.* **2015**, *92*, 104.
28. Kumar, R.; Chopra, R.; Singh, G.; *J. Mol. Liq.* **2017**, *241*, 9.
29. Hegazy, M. A.; Hasan, A. M.; Emara, M. M.; Bakr, M. F.; Youssef, A. H.; *Corros. Sci.* **2012**, *65*, 67.
30. Zhang, B.; He, C.; Wang, C.; Sun, P.; Li, F.; Lin, Y.; *Corros. Sci.* **2015**, *94*, 6.
31. Salhi, A.; Tighadouini, S.; El-Massaoudi, M.; Elbelghiti, M.; Bouyanzer, A.; Radi, S.; El Barkany, S.; Bentiss, F.; Zarrouk, A.; *J. Mol. Liq.* **2017**, *248*, 340.
32. Bellezze, T.; Giuliani, G.; Viceré, A.; Roventi, G.; *Corros. Sci.* **2018**, *130*, 12.
33. Gupta, N. K.; Verma, C.; Quhaishi, M. A.; Mukherjee, A. K.; *J. Mol. Liq.* **2016**, *215*, 47.
34. Soliman, S. A.; Metwally, M. S.; Selim, S. R.; Bedair, M. A.; Abbas, M. A.; *J. Ind. Eng. Chem.* **2014**, *20*, 4311.
35. Hamani, H.; Douadi, T.; Daoud, D.; Al-Noaimi, M.; Rikkouh, R. A.; Chafaa, S.; *J. Electroanal. Chem.* **2017**, *801*, 425.
36. Fouda, A. S.; Ismail, M. A.; EL-ewady, G. Y.; Abousalem, A. S.; *J. Mol. Liq.* **2017**, *240*, 372.
37. Li, X.; Deng, S.; Lin, T.; Xie, X.; Du, G.; *Corros. Sci.* **2017**, *118*, 202.
38. Zhou, L.; Lv, Y.-L.; Hu, Y.-X.; Zhao, J.-H.; Xia, X.; Li, X.; *J. Mol. Liq.* **2018**, *249*, 179.
39. Ansari, K. R.; Quraishi, M. A.; *J. Ind. Eng. Chem.* **2014**, *20*, 2819.
40. Ansari, K. R.; Quraishi, M. A.; Singh, A.; *J. Ind. Eng. Chem.* **2015**, *25*, 89.
41. Döner, A.; Kardas, G.; *Corros. Sci.* **2011**, *53*, 4223.
42. Shukla, S. K.; Quraishi, W. A.; *Corros. Sci.* **2009**, *51*, 1007.
43. Murthy, Z. V. P.; Vijayaragavan, K.; *Green Chem. Lett. Rev.* **2014**, *7*, 209.
44. Villamil, R. F. V.; Corio, P.; Rubim, J. C.; Agostinho, S. M. L.; *J. Electroanal. Chem.* **1999**, *472*, 112.
45. Villamil, R. F. V.; Corio, P.; Rubim, J. C.; Agostinho, S. M. L.; *J. Electroanal. Chem.* **2002**, *535*, 75.
46. Karthikaiseelvi, R.; Subhashini, S.; *Arabian J. Chem.* **2017,** *10***,** S627.

47. Verma, C.; Quhaishi, M. A.; Singh, A.; *J. Mol. Liq.* **2015**, *212*, 804.
48. Dohare, P.; Ansari, K. R.; Quhaishi, M. A.; Obot, I. B.; *J. Ind. Eng. Chem.* **2017**, *52*, 197.
49. Yildiz, R.; Dogan, T.; Dehri, I.; *Corros. Sci.* **2014**, *85*, 215.
50. Ait Albrimi, Y.; Ait Addi, A.; Douch, J.; Souto, R. M.; Hamdani, M.; *Corros. Sci.* **2015**, *90*, 522.
51. Guo, L.; Obot, I. B.; Zheng, X.; Shen, X.; Qiang, Y.; Kaya, S.; Kaya, C.; *Appl. Surf. Sci.* **2017**, *406*, 301.

Submitted: April 10, 2018
Published online: July 11, 2018